Electronic Supplementary Material (ESI) for Soft Matter.

Supplementary Material:

Observation of iron oxide nanoparticle synthesis in magnetogels using magnetic resonance imaging

Samuel D. Oberdick[†‡], *Stephen E. Russek*[‡], *Megan E. Poorman*[†] *and Gary Zabow*[*‡]

[‡]Applied Physics Division

National Institute of Standards and Technology

Boulder, Colorado 80305, USA

[†]Associate of the National Institute of Standards and Technology

Boulder, Colorado 80305, USA

[†]Department of Physics, University of Colorado

Boulder, Colorado 80309, USA

Email: samuel.oberdick@nist.gov, gary.zabow@nist.gov

S1. Calculation of polymer volume fraction and linear mesh size for PEGDMA 1000

The polymer volume fraction is calculated by empirically determining the (mass) degree of swelling

$$q = \frac{m_{swollen}}{m_{dry}} = \frac{0.23\ g}{0.127\ g} = 1.811 \tag{1}$$

which was done by measuring a piece of PEGDMA 1000 when it was dry and then later soaked in a solution of 100 mM elemental iron chloride (2:1 ratio of Fe^{3+} to Fe^{2+}). We then relate this value to the volume fraction of polymer in swollen state using the densities of PEGDMA (1100 kg/m^3)[4] and water (1000 kg/m^3),

$$v_{2,s} = \frac{1/\rho_{PEG}}{(q-1)/\rho_{H_2O}+1/\rho_{PEG}} = \frac{1/(1000\frac{kg}{m^3})}{(1.811-1)/(1000\frac{kg}{m^3})+1/(1100\frac{kg}{m^3})} = 0.58. \tag{2}$$

This method is widely used in literature[5,6,7].

The volume fraction, $v_{2,s,}$ is used to calculated the linear mesh size[8],

$$\xi = {v_{2,s}}^{-1/3} \cdot l \cdot \left(\frac{3C_n\overline{M_c}}{\overline{M_n}}\right)^{1/2} \tag{3}$$

$$\xi = 0.58^{-1/3} \cdot 0.15\ nm \cdot \left(\frac{3 \times 6.9 \times 1000\ Da}{44\ Da}\right)^{\frac{1}{2}} = 2.7\ nm \tag{4}$$

Where l is average bond length (~ 0.15 nm for PEG, assuming carbon-carbon bonds), C_n is the Flory ratio (taken to be 6.9 for PEG based polymers)[9], $\overline{M_n}$ is average molecular weight of the polymer monomer (44 Da for PEG), $\overline{M_c}$ is average molecular weight between crosslinks (simply taken to be 1000 Da, which is the average weight of the monomer used in the experiments).

Once the mesh size has been calculated, we use the Lustig-Peppas estimate of solute diffusivity in swollen gel to determine the diffusion coefficient of hydroxide in the PEGDMA[10,11],

$$D_{OH}^{gel} = D_{OH}^{water} \cdot \left(1 - \frac{R_E}{\xi}\right) \cdot e^{-Y\left(v_{2,s}/(1-v_{2,s})\right)} \quad (5)$$

where D_{OH}^{water} is diffusion coefficient of hydroxide anions in free H_2O (5.27×10^{-9} m^2/s)[12], R_E is the hydrodynamic radius of OH^- (0.11 nm[13]), and Y is critical volume required to successfully translate movement of substrate relative to average free volume of water molecule (taken to be 1 for PEG based gels[11]).

Putting numbers in:

$$D_{OH}^{gel} = 5.27 \times 10^{-9} \frac{m^2}{sec} \times \left(1 - \frac{0.11\ nm}{2.7\ nm}\right) \times e^{-0.58/(1-0.58)} \quad (6)$$

$$= 0.24 \times 5.27 \times 10^{-9} \frac{m^2}{sec}$$

$$= 1 \times 10^{-9} \frac{m^2}{sec}$$

S2. Simulation details

Due to the complexity of the diffusion-reaction dynamics during in situ coprecipitation, numerical simulations were performed to understand the evolution of iron oxide growth within the hydrogel. Simulations were performed using Wolfram Mathematica software (Any mention of commercial products is intended solely for fully detailing research; it does not imply recommendation or endorsement by NIST).

The simulations were performed on a 2D grid and driven by a Monte Carlo like method to model diffusion, which assumed only that random motion of each OH^{-1} ion in each direction was equally likely. Simulations were performed on a 2D cross section of the 3D cylinder (a disc) and integrated to produce results for comparison to experiments. The boundary conditions and initial values were chosen to match those in the experiment. Namely, iron precursor (Fe^{2+} and Fe^{3+}) was confined to a circular region defined by radius = 4 mm. Surrounding the Fe precursor is a bath of OH^{-1} with a concentration 10x higher than the Fe. At each time step, the hydroxide can advance some length based on a random walk and the chosen diffusion coefficient, D_{OH}, which serves as the only free parameter in the model. After each step, OH^{-1} and Fe units that are co-located are converted to iron oxide according to the necessary 3:8 ratio for $Fe:OH^{-1}$, which is set by the basic reaction equation for co-precipitation (Equation 1, main paper). Any Fe and OH^{-1} ions converted in this way are removed from the simulation and replaced by a spatially fixed amount of iron-oxide, determined again by the above ratio.

The reaction-diffusion character of *in situ* coprecipitation has dynamics that are distinct from a simpler, diffusion driven system. This is especially apparent when looking at the effect of different initial conditions. By choosing different initial values for the ratio of Fe precursor in the gel to the concentration of OH^{-1} in the surrounding bath, the reaction rate changes markedly. This is displayed in Figure S1, which only shows a diffusion-like curve for OH^{-1} ions at very high ratios of OH^{-1} to Fe ions. In this case, elimination of OH^{-1} ions due to the precipitation reaction becomes negligible compared to their overall number.

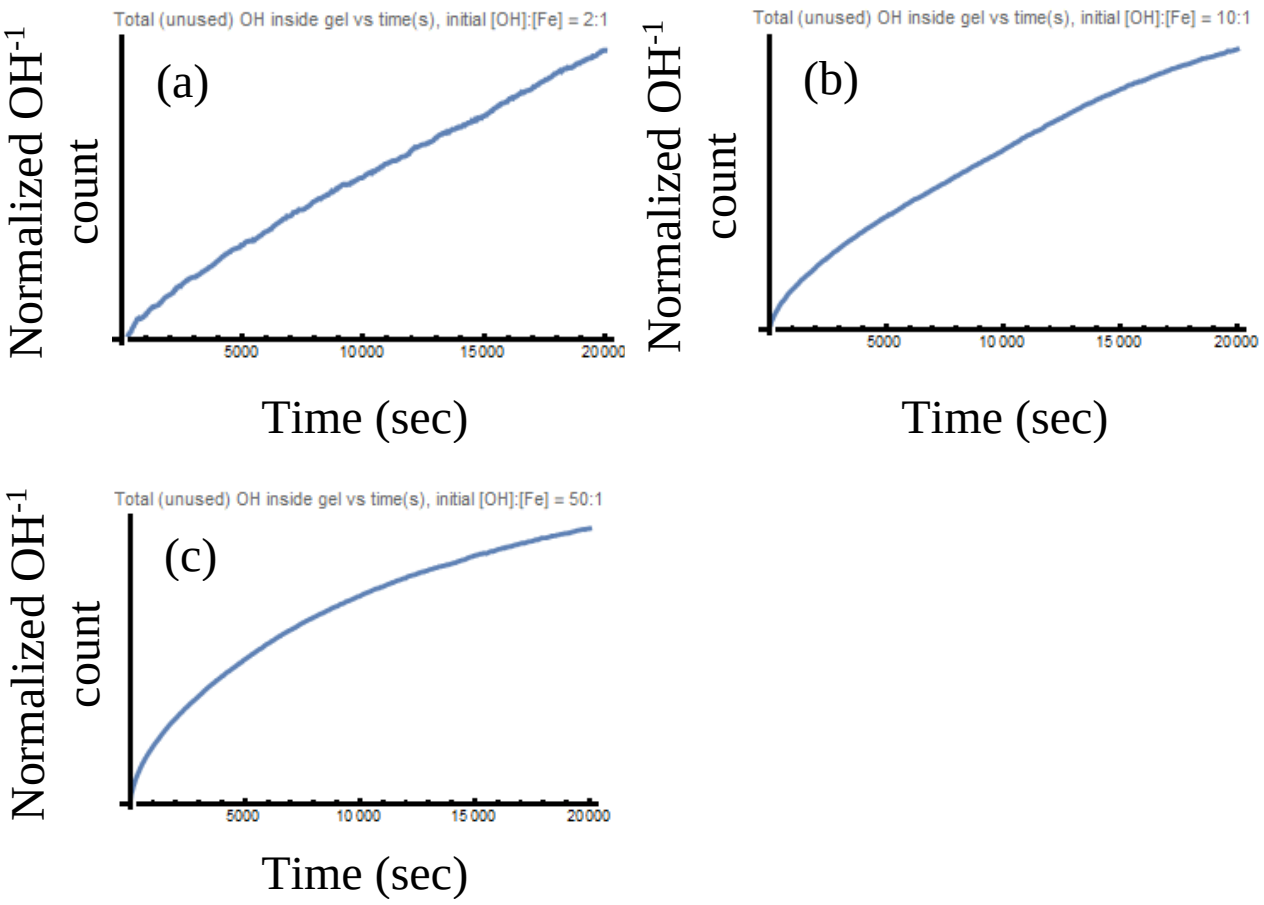

Figure S1. Normalized number of hydroxide ions that have diffused into the gel as a function of time for (a) 2:1 ratio of [OH^{-1}]:[Fe] (b) 10:1 ratio of [OH^{-1}]:[Fe] and (c) 50:1 ratio of [OH^{-1}]:[Fe].

S3. Calculation of iron oxide nanoparticle diameter from Langevin fit to *M-H* curve

The magnetic moment of a small, dry piece of magnetogel was measured as a function of field from -7 T to 7 T. The sample had a mass of 16.3 mg and was prepared with 100 mM elemental iron as a precursor (2:1 ratio of Fe^{3+}:Fe^{2+}). The diamagnetic contribution from the polymer network was corrected by fitting high field data to a line, and then subtracting the linear background from the original data. The data was then fit to a Langevin function of the form,

$$M(\alpha H) = M_0 \left(\coth(\alpha H) - \frac{1}{\alpha H} \right) \tag{7}$$

with the variable α is given as,

$$\alpha = \frac{\mu}{k_B T} \tag{8}$$

where M_0 is the saturation magnetization of the sample, H is the applied field, μ is the magnetic moment of a single iron oxide nanoparticle, k_B is Boltzmann's constant and T is the temperature. If we assume that the particles have a spherical shape and uniform density, then α can be expressed as,

$$\alpha = \frac{\mu}{k_B T} = \frac{M_s V}{k_B T} = \frac{M_s}{k_B T} \cdot \frac{4}{3} \pi r^3 \tag{9}$$

where M_s is the (volume) magnetization of the iron oxide nanoparticles and V is the volume of the particles (equal to $4/3\pi r^3$ if spherical). The fit of the data is displayed in Figure S3. The fit gives α = 12.6. Rearranging Equation 9 to express r in terms of the other parameters gives,

$$r = \left(\frac{3\alpha k_B T}{4\pi M_s} \right)^{1/3}. \tag{10}$$

Finally, we evaluate Equation 10 using a temperature of 300 K and the saturation magnetization of magnetite (480 kA/m)[14], we calculate that $r = 3 \times 10^{-9}$ m. The diameter, then, is roughly 6 nm.

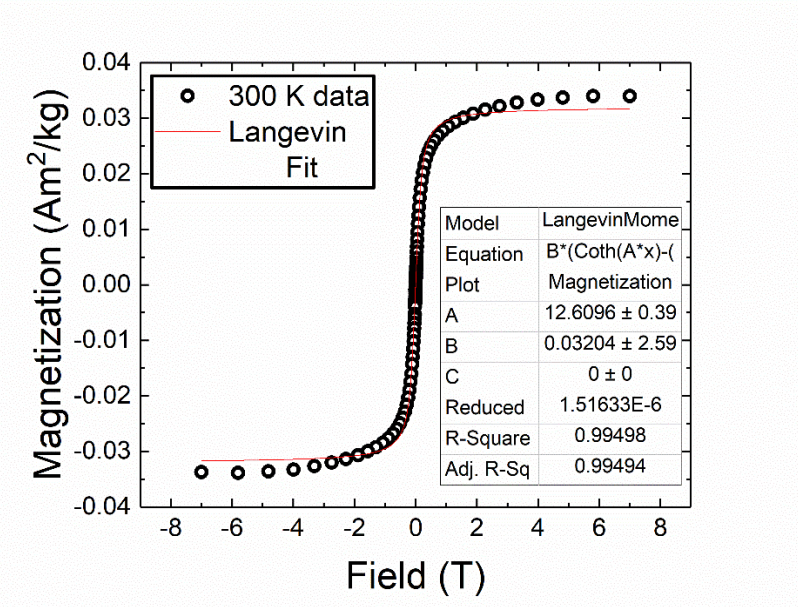

Figure S2. *M-H* curve from magnetogel fit to a single Langevin function.

S4. Estimation of both mass and volume fraction of iron oxide nanoparticles

The saturation magnetization (mass) of the sample measured in Figure S1 is ~0.033 Am^2/kg. If the sample were made entirely of magnetite, its saturation magnetization would be 92 Am^2/kg at 300 K[14]. This means that the mass fraction of iron oxide in the sample is 0.033/92 = 0.0004.

We can calculate the volume fraction of iron oxide in terms of the total sample mass, m_{sample}, the mass of iron oxide in the sample, m_{Fe3O4}, and densities of iron oxide (5170 kg/m^3) and PEGDMA (1100 kg/m^3). The mass of the sample was 16.3 mg. The mass of iron oxide was found by taking the magnetic moment at 7 T (5.54×10^{-7} Am^2) and dividing by the saturation magnetization (mass) of magnetite at 300 K (92 Am^2/kg). This gives m_{Fe3O4}= (5.54×10^{-7} Am^2) / (92 Am^2/kg) = 6×10^{-9} kg. The volume fraction of magnetite can then be calculated,

$$\varphi = \frac{volume_{Fe3O4}}{volume_{Fe3O4} + volume_{PEGDMA}} = \frac{m_{Fe3O4}/\rho_{Fe3O4}}{\frac{m_{Fe3O4}}{\rho_{Fe3O4}} + \frac{m_{sample} - m_{Fe3O4}}{\rho_{PEGDMA}}} = 0.00007. \quad (11)$$

S5. Calculation of magnetic diameter of iron oxide from ZFC/FC curves

The nanoparticle diameters were estimated from blocking temperature, T_B, by setting the Neél relaxation time equal to a characteristic measurement time, τ_m. This results in a well-recognized expression for blocking temperature,

$$T_B = \frac{KV}{k_B \ln\left(\frac{\tau_m}{\tau_0}\right)} \tag{12}$$

where K is the effective magnetic anisotropy of the particles, k_B, is Boltzmann's constant and τ_0 is the characteristic attempt time for magnetization reversal (usually taken to be 10^{-9} s). Assuming spherical geometry (volume equal to $4/3\pi r^3$), we can solve for the radius, r,

$$r = \left(\frac{3}{4\pi}\frac{k_B T_B \ln\left(\tau_m/\tau_0\right)}{K}\right)^{\frac{1}{3}}. \tag{13}$$

The blocking temperature for each molecular weight is using the inflection point to the left of the peak in the ZFC curve[15]. These values are $T_{B,1k}$ ~ 7.5 K and $T_{B,8k}$ ~ 49.9 K. The anisotropy is taken to be that of bulk magnetite, K = 13.5 kJ/m^3.[15] During the measurement, the temperature was swept at 5 K/minute and from 2 K up to 300 K. The applied magnetic field was 0.001 T. The time for a DC measurement at a single temperature was on the order of 10 seconds, meaning that $\ln(\tau_m/\tau_0) = \ln(10/10^{-9}) \sim 18$. These values can be used with Equation 13 to calculate the radius of nanoparticles within the PEGDMA 1000 and PEGDMA 8000 composites. They are found to be r_{1k} = 3.2 nm and r_{8k} = 6 nm.

REFERENCES

(1) Crank, J. *The Mathematics of Diffusion*; Clarendon Press, 1975.
(2) Crank, J.; Park, G. S. *Diffusion in Polymers*; Academic Press: London, 1968.
(3) Buckley, D. J.; Berger, M. The Swelling of Polymer Systems in Solvents. II. Mathematics of Diffusion. *Journal of Polymer Science* **1962**, *56* (163), 175–188. https://doi.org/10.1002/pol.1962.1205616315.
(4) Polyethylene glycol dimethacrylate (PEGDMA 1000) https://www.polysciences.com/default/catalog-products/polyethylene-glycol-dimethacrylate-pegdma-1000 (accessed Jan 29, 2020).
(5) Evans, S. M.; Litzenberger, A. L.; Ellenberger, A. E.; Maneval, J. E.; Jablonski, E. L.; Vogel, B. M. A Microfluidic Method to Measure Small Molecule Diffusion in Hydrogels. *Materials Science and Engineering: C* **2014**, *35*, 322–334. https://doi.org/10.1016/j.msec.2013.10.035.
(6) Durmaz, S.; Fank, S.; Okay, O. Swelling and Mechanical Properties of Solution-Crosslinked Poly(Isobutylene) Gels. *Macromolecular Chemistry and Physics* **2002**, *203* (4), 663–672. https://doi.org/10.1002/1521-3935(20020301)203:4<663::AID-MACP663>3.0.CO;2-W.
(7) Peppas, N. A.; Huang, Y.; Torres-Lugo, M.; Ward, J. H.; Zhang, J. Physicochemical Foundations and Structural Design of Hydrogels in Medicine and Biology. *Annual Review of Biomedical Engineering* **2000**, *2* (1), 9–29. https://doi.org/10.1146/annurev.bioeng.2.1.9.
(8) Slaughter, B. V.; Khurshid, S. S.; Fisher, O. Z.; Khademhosseini, A.; Peppas, N. A. Hydrogels in Regenerative Medicine. *Advanced Materials* **2009**, *21* (32–33), 3307–3329. https://doi.org/10.1002/adma.200802106.
(9) Characteristic Ratio http://polymerdatabase.com/polymer%20physics/C%20Table2%20.html (accessed Jan 29, 2020).
(10) Amsden, B. Solute Diffusion within Hydrogels. Mechanisms and Models. *Macromolecules* **1998**, *31* (23), 8382–8395. https://doi.org/10.1021/ma980765f.
(11) Lustig, S. R.; Peppas, N. A. Solute Diffusion in Swollen Membranes. IX. Scaling Laws for Solute Diffusion in Gels. *Journal of Applied Polymer Science* **1988**, *36* (4), 735–747. https://doi.org/10.1002/app.1988.070360401.
(12) Henry, V. K. (Ed.). *CRC Handbook of Thermophysical and Thermochemical Data.*; CRC Press Inc.: Boca Raton, 1994.
(13) Marcus, Y. Volumes of Aqueous Hydrogen and Hydroxide Ions at 0 to 200 °C. *J. Chem. Phys.* **2012**, *137* (15), 154501. https://doi.org/10.1063/1.4758071.
(14) Cullity, B. D.; Graham, C. D. *Introduction to Magnetic Materials*; John Wiley & Sons, 2011.
(15) Livesey, K. L.; Ruta, S.; Anderson, N. R.; Baldomir, D.; Chantrell, R. W.; Serantes, D. Beyond the Blocking Model to Fit Nanoparticle ZFC/FC Magnetisation Curves. *Sci Rep* **2018**, *8* (1), 11166. https://doi.org/10.1038/s41598-018-29501-8.